REGULAR ARTICLE

Validation of organotypical hippocampal slice cultures as an ex vivo model of brain ischemia: different roles of NMDA receptors in cell death signalling after exposure to NMDA or oxygen and glucose deprivation

Hanna Ahlgren · Kristi Henjum · Ole Petter Ottersen · Elise Rundén-Pran

Abstract *N*-Methyl-D-aspartate receptors (NMDARs) are essential mediators of synaptic plasticity under normal physiological conditions. During brain ischemia, these receptors are excessively activated due to glutamate overflow and mediate excitotoxic cell death. Although organotypical hippocampal slice cultures are widely used to study brain ischemia in vitro by induction of oxygen and glucose deprivation (OGD), there is scant data regarding expression and functionality of NMDARs in such slice cultures. Here, we have evaluated the contribution of NMDARs in mediating excitotoxic cell death after exposure to NMDA or OGD in organotypical hippocampal slice cultures after 14 days in vitro (DIV14). We found that all NMDAR subunits were expressed at DIV14. The NMDARs were functional and contributed to cell death, as evidenced by use of the NMDAR antagonist MK-801 (dizocilpine). Excitotoxic cell death induced by NMDA could be fully antagonized by 10 μM MK-801, a dose that offered only partial protection against OGD-induced cell death. Very high concentrations of MK-801 (50–100 μM) were required to counteract cell death at long delays (48–72 h) after OGD. The relative high dose of MK-801 needed for long-term protection after OGD could not be attributed to down-regulation of NMDARs at the gene expression level. Our data indicate that NMDAR signaling is just one of several mechanisms underlying ischemic cell death and that prospective cytoprotective therapies must be directed to multiple targets.

Keywords Organotypical hippocampal slice cultures · NMDA receptors · Excitotoxicity · Ischemia · Oxygen and glucose deprivation (OGD)

H. Ahlgren · K. Henjum · O. P. Ottersen · E. Rundén-Pran
Center for Molecular Biology and Neuroscience
and Department of Anatomy, Institute of Basic Medical Sciences,
University of Oslo,
0317 Oslo, Norway

H. Ahlgren
Department of Neurobiology, Interdisciplinary
Center for Neurosciences (IZN), University of Heidelberg,
Heidelberg, Germany

E. Rundén-Pran (✉)
Health Effects Laboratory, Department of Environmental
Chemistry, NILU- Norwegian institute for Air Research,
2027 Kjeller, Norway
e-mail: erp@nilu.no

Introduction

N-Methyl-D-aspartate receptors (NMDARs) are a class of glutamate-activated cationotropic receptors that are highly permeable to Ca^{2+} and Na^+. Influx of ions upon activation contributes to membrane depolarization and intracellular Ca^{2+} transients that are responsible for the physiological effects of NMDAR signaling. NMDARs are essential mediators of synaptic plasticity both in the developing and adult brain (Aamodt and Constantine-Paton 1999; Bliss and Collingridge 1993; Malenka and Nicoll 1999). They are most likely heterotetramers, composed of two NR1 subunits and two glutamate-binding NR2 subunits that are encoded by four different genes (NR2A-D) (Monyer et al. 1992). In some cases, NMDARs also contain NR3 subunits (Moriyoshi et al. 1991; Szydlowska and Tymianski 2010). The most commonly expressed NMDAR in the mammalian central nervous system (CNS) consists in two obligatory NR1 subunits in combination with either NR2A and/or NR2B (Kohr 2006). The NR2A and NR2B subunits display

different expression patterns during development: the NR2B subunit is expressed already at early developmental stages, whereas NR2A appears after birth (Gambrill and Barria 2011). For either subunit the expression peaks around postnatal day 20 (Kohr 2006; Monyer et al. 1994; Sheng et al. 1994). The C-terminal domains of the NMDAR subunits mediate coupling to distinct downstream signaling pathways involved both in physiological and pathophysiological responses (Szydlowska and Tymianski 2010).

During pathophysiological conditions, such as in brain ischemia, lack of energy induces a collapse of ionic gradients followed by excessive neuronal depolarization, release of excitatory neurotransmitters and reduced re-uptake of neurotransmitters from the extracellular space. Glutamate is the major excitatory neurotransmitter in the mammalian brain and increased level of glutamate, as occurs in stroke, induces overstimulation of NMDARs, massive influx of Ca^{2+} and activation of cell death signaling pathways (Arundine and Tymianski 2003; Choi 1992; Lipton and Rosenberg 1994). This overstimulation of NMDARs is referred to as excitotoxicity and is assumed to account for much of the neurodegeneration that occurs after an ischemic insult in vivo (Olney 1969). However, recent data have revealed that NMDAR-induced damage is a more complex phenomenon than previously assumed, calling for a re-examination of the roles of NMDARs in brain ischemia. Several studies indicate that the involve-ment of NMDARs in ischemic cell death signaling depends on receptor localization (extrasynaptic versus synap-tic) (Hardingham et al. 2002; Zhang et al. 2007; 2011) or subunit-composition (NR2A vs NR2B) (Liu et al. 2007). Synaptic NMDARs are claimed to mainly activate signaling cascades and genes promoting cell survival, whereas the extrasynaptic NMDARs are thought to activate signaling cascades and genes that promote cell death (Hardingham and Bading 2010; Milnerwood et al. 2010). Other reports suggest that both pools of NMDARs (extrasynaptic and synaptic) can participate in excitotoxic cell death signalling (Sattler et al. 2000; Stanika et al. 2009) and that the subunit composition determines if cell survival (NR2A) or cell death (NR2B) signaling cascades are activated (Martel et al. 2009).

Brain ischemia can be studied in vitro in dispersed neuronal cultures as well as in organotypical slice cultures by bath application of NMDAR agonists or by induction of OGD (Laake et al. 1999; Runden-Pran et al. 2002, 2005; Ring et al. 2010; Bonde et al. 2005; Noraberg et al. 2007). In organotypical slice cultures the cytoarchitecture is retained. Notably, connections between hippocampal sub-regions CA1, CA3 and the dentate gyrus (DG) are intact (Gähwiler et al. 1997). The maintenance of glial–neuronal interactions is important when investigating pathophysio-logical conditions like ischemia, where impaired glutamate

uptake by glial cells could contribute to increased extracel-lular level of glutamate and induction of excitotoxicity (Benveniste et al. 1984; Camacho and Massieu 2006; Rossi et al. 2000). The organotypical model offers an alternative to dissociated cell cultures and in vivo models, allowing investigation of molecular mechanisms underlying excito-toxic cell death signaling without perturbation due to systemic parameters (Noraberg et al. 2007; Bonde et al. 2005; Ring et al. 2010; Laake et al. 1999; Runden-Pran et al. 2002, 2005; Rolseth et al. 2008; Cook and Tymianski 2011).

NMDARs contribute to cell death in organotypical slice cultures subjected to OGD (Bonde et al. 2005; Kristensen et al. 2001; Martinez-Sanchez et al. 2004; Montero et al. 2007; Newell et al. 1995; Noraberg et al. 2007). They also mediate cell death in acute brain slices (Zhou and Baudry 2006). However, no comparative analysis has been per-formed on NMDA- and OGD-evoked cell death in such cultures, nor on the contribution of NMDARs in these different experimental paradigms. Such data are urgently needed to justify extrapolations to the conditions that prevail during stroke. Furthermore, information is scant regarding the expression of NMDARs in organotypical hippocampal slice cultures in parallel to in vivo hippocam-pal expression at a corresponding age. Given the distinct developmental profile of NMDAR subunits, one cannot assume, a priori, that slices harvested from newborn rats display the same complement of receptors as that seen in mature animals used in in vivo stroke models. Therefore, in this study, we evaluate the contribution of NMDARs to cell death induced by NMDA or OGD, respectively. We also characterize the developmental expression of NMDAR subunits NR1, 2A and 2B in organotypical hippocampal slices and directly compare the expression pattern with that seen in situ.

Materials and methods

Materials

Culture media were from GIBCO (Life Technologies, Paisley, UK) and other chemicals used were from Sigma-Aldrich (Norway) unless otherwise indicated.

Preparation of organotypical hippocampal slice cultures

Organotypical hippocampal slice cultures were prepared as previously described (Runden et al. 1998; Rolseth et al. 2008). Both hippocampi were quickly dissected under aseptic conditions from postnatal 5 or 6 days old Wistar rats (M&B, Taconic, Denmark). The hippocampi were then cut into 350- to 375-μm-thick transverse slices with a

McIlwain tissue chopper and immediately transferred for separation into Gey's balanced salt solution (GBSS) (1.5 mM $CaCl_2$, 5 mM KCl, 0.22 mM KH_2PO_4, 1 mM Mg Cl_2, 0.3 mM $MgSO_4$, 137 mM NaCl, 2.7 mM $NaHCO_3$, 1 mM Na_2HPO_4, 5.6 mM D-glucose) supplemented with 5 mg/ml glucose. Hippocampal slices with intact subregions and fimbria were individually placed on glass cover slips (Kindler, Freiburg, Germany) with chicken plasma. Thrombin (from bovine plasma; Merck, Germany) diluted in GBSS/ultra-pure H_2O was added in order to attach the slice to the cover slip by clot formation. The slices were then transferred to flat-sided culture tubes (Nunc; Nalge Nunc International, Nagerville, USA) containing 750 μl culture media composed of 50% Basal medium Eagle (with Hanks' salts, BME; BioConcept, Switzerland), 25% Hanks' balanced salts (HBSS, GIBCO), 25% horse serum (GIBCO) and supplemented with 100U/ml Penicillin G, 100 μg/ml streptomycin (Invitrogen or GIBCO), 1 mM L-glutamine and 20 mM glucose and cultivated in a roller drum on a rotator (Bellco Biotechnology, NJ, USA) tilted at an angle of 5º, rotating with a speed of ~8 rph in an incubator at 36°C. The culture medium was changed after 1 week and the cultures were grown for 2 weeks prior to experiments. Efforts were made to reduce the number of animals used in accordance with the European Communities Council directive 86/609/EEC.

Oxygen and glucose deprivation (OGD)

OGD was induced as previously described (Laake et al. 1999) with some modifications (Rytter et al. 2003). Prior to an experiment, the slice cultures were incubated overnight with propidium iodide (PI) (5 μg/ml dissolved in dimethyl sulfoxide (0.001% DMSO)) added to the culture medium. Slice cultures showing a distinct uptake of PI in the pyramidal cell layer were excluded. PI is a fluorescent dye that binds to nucleic acid in cells with a damaged cell membrane and is used as an indicator of cell death (Laake et al. 1999; Noraberg et al. 1999). During an experiment, PI was included in all solutions used unless stated otherwise. On the experimental day, the slice cultures were pre-incubated for 60 min in a culture medium with MK-801 or solvent alone. After pre-incubation, the slice cultures in the OGD group were washed once with ischemic cerebral spinal fluid solution (iCSF) (0.3 mM $CaCl_2$, 70 mM NaCl, 5.25 mM $NaHCO_3$, 70 mM KCl, 1.25 mM NaH_2PO_4, 2 mM $MgSO_4$, 20 mM sucrose), pre-bubbled with an anoxic gas mixture (80% N_2, 10% H_2 and 10% CO_2), to get rid of oxygen and acidify the solution to pH 6.5-6.8. The slice cultures were then transferred to an anaerobic incubator with custom-made modifications (Electrotec workstation, mini, Sweden) with the same gas mixture and a temperature set to 36°C. Traces of oxygen were removed by a palladium catalyst and stable anaerobic conditions were monitored with an oxygen indicator solution. In the anaerobic incubator the slice cultures were washed once more with iCSF before adding either iCSF solely (control) or the NMDA-receptor antagonist MK-801 (10, 50, 100 μM) or NMDA (200 μM) diluted in iCSF and placed for 15 min in a roller drum on a rotator (Bellco Biotechnology) (see above). After the ischemic insult, the slice cultures were removed from the anaerobic incubator, washed twice with the culture medium and incubated for up to 72 h with either a culture medium or a culture medium supplemented with MK-801 at the same concentrations as above. The control slice cultures (no OGD) were washed twice with artificial cerebral spinal fluid solution (aCSF) (2 mM $CaCl_2$, 125 mM NaCl, 25 mM $NaHCO_3$, 2.5 mM KCl, 1.25 mM NaH_2PO_4, 2 mM $MgSO_4$, 20 mM glucose, pH ~7.4) and incubated throughout the experiment with aCSF in a standard aerobic incubator in a roller drum. At the end of an experiment, the control slices were also washed twice with a culture medium, added fresh culture medium and evaluated for cell death at defined time points up to 72 h without further change of media (as roller drum slice cultures normally get new media only once a week). For evaluation of development of cell death, recordings were made up to 144 h after OGD.

NMDA-induced cell death

NMDA-induced cell death was achieved by incubating the slice cultures with NMDA (150 μM) diluted in aCSF for 15 min in a standard aerobic incubator. Pre-selection of viable slice cultures, pre-incubation with MK-801 (10, 50, 100 μM), control slices and the termination of the experiments were performed according to the OGD-protocol described above. The slice cultures were evaluated for cell death at defined time-points up to 72 h after exposure with no further change of media.

Quantification of cell death

Quantification of cell death was performed as described previously (Runden-Pran et al. 2005). Cell death was assessed by measuring the PI-fluorescence before OGD or exposure to NMDA (0 h) and at different time-points (24, 48 and 72 h) following the insults. Slice cultures were examined with an inverted Olympus IMT2 microscope with a ×4 objective and ×2.5 ocular and images were captured with a C4880-96 cooled CCD camera driven by the manufacturer's software (Hamamatsu HiPic 4.2.1). PI-fluorescence was induced with light from a 100-W mercury lamp, attenuated with a grey-filter and passed through a rhodamine filter cube (Olympus IMT2-DMG). Illumination, integration time and camera gain were set to fully

exploit the 12-bit intensity range of the imaging system without saturating it and were kept throughout the experiment nominally constant for all images at each time-point. Each series of recording was started by recording a dark current image with the chosen integration time and camera gain but with a closed light path (camera temperature −30°C). Also, a shading correction image was recorded from a preparation of PI dissolved in DMSO (2.5 mg/ml). Shading correction was performed to correct for spatially non-uniform sensitivity of the complete imaging system. PI fluorescence was evaluated with the image processing software analySIS (Soft Imaging Software, Münster, Germany). For semi-quantitative analysis, freehand regions of interest (ROIs) were created around the dentate gyrus (DG) and the CA3 and CA1 hippocampal subfields of each slice culture. The mean grey-values for each ROI (per unit area) were calculated from the fluorescence intensity and imported into the SPSS statistical software (SPSS, USA). We have earlier shown that there is a good correlation between the number of dead cells and the PI-fluorescence intensity. The auto-fluorescence and unspecific accumulation of PI in the tissue were corrected by subtracting the grey-values from the images at 0 h from the grey-values of the same cultures at 24, 48 and 72 h after the insults, i.e. each slice was normalized to itself using this method (for Fig. 4, the analysis were performed at 2, 4, 6, 10, 12, 24, 48, 72, 96, 120 and 144 h after OGD). The statistical analyses were performed with the non-parametric Kruskall-Wallis test for comparison of differences between all groups and one-tailed non-parametric Mann–Whitney U test for comparison of paired groups. Data are presented as means ± SEM.; $P<0.05$ was considered statistically significant.

Sample collection for Western blotting

For comparative developmental immunoblot analysis of protein expression levels, the whole hippocampal formation was studied at postnatal day (P) 6, 12, 19 and 26, whereas slice cultures were studied at corresponding developmental stages: days in vitro (DIV) 0 (on the same day the slice was prepared), 7, 14 and 21. Slice cultures from four to five different animals ($n=4$–5) were pooled at each time point and immediately snap frozen in liquid nitrogen. Whole hippocampi from two rat pups ($n=2$) at each time point as well as whole hippocampi and cortex from adult mouse and rat were dissected in an ice-cold GBSS buffer and snap frozen in liquid nitrogen. Forebrain tissue from adult NR2A$^{−/−}$ and NR2B$^{\Delta f}$ knock out (KO) mice and their wild-type (WT) mice was collected immediately after preparation of acute hippocampal slices and snap frozen in liquid nitrogen. NMDAR2B conditional KO mice were generated with the Cre/loxP system to target NR2B gene deletion in principal neurons of the postnatal brain

(NR2B$^{\Delta Fb}$). The NR2B exon 9 was flanked by loxP sites (NR2B^{2lox} mice) and GABAergic interneurons are spared as they do not express α-CaMKII promoter-driven Cre (Sakimura et al. 1995; von Engelhardt et al. 2008).

Immunoblot analysis

Slice cultures were homogenized by sonication and whole hippocampi with a pestle, on ice in an RIPA-lysis buffer (1 mg tissue/10 μl lysis buffer) (0.1% SDS, 1% Triton-X-100, 0.5% DOC (deoxycholic acid), 50 mM Tris (pH 7.4), 150 mM NaCl, 5 mM EDTA, protease inhibitor cocktail (Roche)). After homogenization, the samples were centrifuged and the supernatant was collected into new tubes. The total protein concentration was measured with a detergent-compatible DC-Kit (Bio-Rad) and a microplate reader (Bio-Rad Benchmark) at 622 nm. The samples were diluted in a 6× sample loading buffer (1× sample loading buffer contained 1.7% SDS, 60 mM Tris-HCl pH 6.8, 5% glycerol, 100 mM DTT and a trace amount of bromophenol blue) to reach a final concentration of 1 μg/μl. Twenty μg of protein were applied per well on a pre-cast Tris-HCl 4-20% gradient gel (Criterion; Bio-Rad), separated under denaturing conditions and thereafter transferred onto a polyvinylidene difluoride (PVDF) membranes (BioRad). PVDF membranes were incubated for 1–2 h in a blocking buffer [5% non-fat milk in Tris buffered saline (137 mM NaCl, 20 mM Tris, pH 7.6) containing 0.05% Tween (TBS-T)] and then overnight with primary antibodies against: rabbit-anti-NR1 (Chemicon 1:800), mouse-anti-NR1 (BD Pharmingen 1:800), rabbit-anti-NR2A (Chemicon 1:300), rabbit-anti-NR2B (Novus Biological 1:300) and rabbit-anti-β-actin (Sigma-Aldrich 1:500). Membranes were then rinsed 3× in TBS-T and incubated with secondary antibodies; either with peroxidase-labeled anti-rabbit or anti-mouse (Sigma-Aldrich) for 1–1.5 h. After washes with TBS-T, the membranes were incubated for 10 min with Enhanced Chemi-Fluorescence (ECF)-substrate (Amersham Biosciences) to elicit a fluorescent signal that was scanned on a Typhoon 9410 scanner (Amersham Biosciences) at 532 nm.

RNA isolation, cDNA synthesis and TaqMan realtime PCR

For TaqMan real-time PCR studies, slice cultures from four to five different animals ($n=4$–5) were collected at different time points after OGD (1, 3, 4, and 24 h), pooled and stored in RNAlater (Ambion) at −20°C. The RNA isolation was performed with an RNeasy RNA isolation kit (Qiagen) and the DNAse treatment with an RNase-free DNase set (Qiagen) according to the manufacturer's

instructions. The RNA concentration was quantified using NanoDrop (NanoDrop Technologies, Wilmington, USA) UV spectrometry and RNA with the A_{260}/A_{280} ratio 1.9–2.1 was converted further into cDNA (0.04 μg RNA/μl reaction) using the High Capacity cDNA Archive Kit (Applied Biosystems). The expression of different NMDAR subunits was measured using TaqMan assays: Rn01436034_m1 (NR1, all splice variants), Rn01424654_m1 (NR2A) and Rn00680474_m1 (NR2B) (Applied Biosystems) and standardized to rGAPDH (Rn99999916_s1) control, on a 7900 HT Fast Real-Time PCR System (Applied Biosystems).

Results

Expression of NMDAR subunits NR1, NR2A and NR2B in DIV14 organotypical slice cultures is comparable to expression *in situ*

We wanted to compare the expression profile of the NMDAR subunits NR1, NR2A and NR2B in organotypical hippocampal slice cultures with the developmental expression of these receptor subunits in hippocampus in situ. For organotypical slice cultures to serve as a good model for studying excitotoxic cell death signaling, the receptor expression pattern in slices should match the expression pattern in situ.

Expression levels of NR1, NR2A and NR2B were assessed in slice cultures at different days in vitro (DIV0, DIV7, DIV14 and DIV21) and in freshly dissected rat hippocampi at corresponding postnatal days (P6, P12, P19 and P26). Organotypical slice cultures were prepared from P6 rat pups (corresponding to DIV0 in vitro) and grown for 2 weeks until DIV14. After preparation, the slice cultures were allowed to recover for 6 h in the incubator at 36°C before being subjected to further analysis.

We found that from DIV7 to DIV21 (corresponding to P14 and P26), the protein levels of NR1, NR2A and NR2B in slice cultures were strikingly similar to the protein levels in situ (Fig. 1a–c).

The expression of the NR1 subunit was investigated with two antibodies recognizing two different NR1 subunit epitopes. The BD Pharmingen NR1 antibody recognizes an extracellular epitope, while the Chemicon NR1 antibody recognizes an intracellular epitope. Both antibodies indicated the same NR1 expression pattern and protein levels, in vitro as well as in situ (Fig. 1a). NR1 was strongly expressed throughout development both in the slice cultures and in hippocampus in situ (Fig. 1a). The most striking in vitro result was the pronounced reduction of protein levels for all the NMDAR subunits and to some extent also for β-actin, on the day the slice cultures were prepared (DIV0; cf. levels at P6). From DIV0 to DIV21, there was a steady increase in receptor protein levels.

NR2A displayed a gradual upregulation with age in the slice cultures as well as in situ (Fig. 1b). Characteristic of the in situ situation was the appearance of three high-molecular weight (MW) bands for NR2B. The relative density of these bands changed with age, with the lowest MW band at ~140 kDa being predominant at P6 and the highest band at ~180 kDa being predominant at P19 and P26 (Fig. 1c). In the slice cultures, the highest band at ~180 kDa was dominant at all DIV investigated, with only indistinct bands at lower molecular weights. Thus, for NR2B, the expression pattern in slice cultures reflected the mature pattern in situ.

Antibody specificity for the NR2 subunits was tested in adult mice with either global deletion of the gene encoding NR2A ($NR2A^{-/-}$) or with conditional deletion of the gene encoding NR2B ($NR2B^{\Delta fb}$). The NR2A signal was abolished in the NR2A KO material (Fig. 2a). For NR2B, a residual signal remained in tissue from the $NR2B^{\Delta fb}$ mice, probably reflecting NR2B in GABAergic interneurons (Sakimura et al. 1995) (Fig. 2b). A so-called mosaic pattern (Clark et al. 1994), including a residual signal, can often be observed in genetically modified mice with a conditional knockout. Each of the three high-MW bands for NR2B was attenuated, indicating that they represent bona fide NR2B immunoreactivity. The three bands obtained with the NR2B antibody were reproduced in extracts from hippocampus and cerebral cortex of both mice and rats (Fig. 2c), ruling out the possibility of species or regional differences.

NMDARs expressed in organotypical hippocampal slice cultures are fully capable of inducing excitotoxic cell death at DIV14

We exposed slice cultures to high concentrations of NMDA (150 μM) to induce excitotoxicity (Fig. 3). NMDA induced cell death in all hippocampal subregions and cell death could be counteracted by the open channel blocker MK-801 (10, 50, or 100 μM) at all time points after the insult (Fig. 3a–c). MK-801 fully antagonized NMDA-induced cell death in CA1, CA3 and DG, even at the lowest concentration used (10 μM) (Fig. 3a–c).

MK-801 only partially counteracted excitotoxic cell death induced by oxygen and glucose deprivation (OGD) in organotypical hippocampal slice cultures

In our model, OGD induces selective and delayed cell death in the vulnerable CA1 pyramidal cells, reflecting the in vivo situation in stroke. Cell death in CA1 appears around 24 h after OGD and increase with time to reach a maximum around 72 h after the insult (Fig. 4).
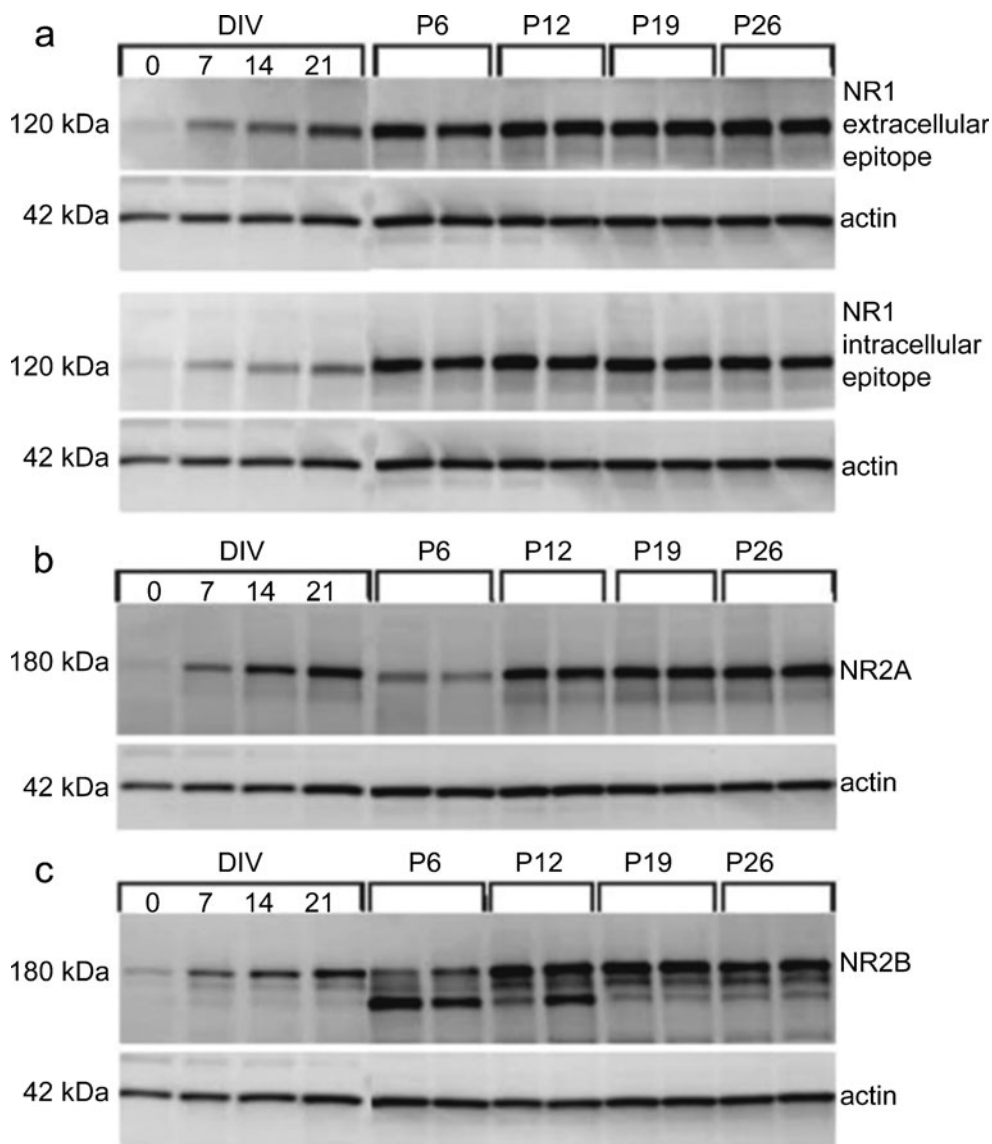
Fig. 1 NMDA receptor subunit expressions in vitro and in situ-time course a comparison between hippocampal organotypical slice cultures and rat pup hippocampi. **a** Western blots from extracts from organotypical hippocampal slice cultures and also from rat hippocampi labeled both with an antibody against an extracellular epitope and with an antibody against an intracellular epitope of the NR1 subunit. Extracts were obtained at different days in vitro (*DIV*) (0–21) from the slice cultures and at corresponding postnatal days (*P*) (6–26) from rat hippocampi. DIV0 was the day of preparation of the slices from P6 animals, corresponding to P6 in situ. β-actin was used as a loading control. NR1 was strongly expressed in situ at all ages analyzed. In the slice cultures, protein levels were strongly decreased at the day of slice preparation and gradually recovered until strongly expressed at DIV14. Both antibodies against the extra- and intracellular epitope of NR1 gave a similar expression pattern, confirming the specificity of the antibody. **b** As in (**a**) but with an antibody against the NR2A subunit. There was an increase in expression of NR2A from P6 to P12 in situ, with a sustained strong expression level. NR2A was also strongly expressed at DIV 21 in vitro in the slice cultures. **c** As in (**a**) but with an antibody against the NR2B subunit. The NR2B antibody gave three bands and there was a shift from strong expression of the lowest band and weak expression of the highest band to the opposite from P6 to P18. In the slice cultures the labeling pattern resembled the mature pattern at all DIV, with strongest expression of the highest band (∼180 kDa) and very indistinct labeling of the lowest band. For in vitro $n=4$–5 animals per group (4–5 slices from 4–5 animals pooled together per group) and in situ $n=2$ animals per group

To evaluate the contribution of the NMDARs in OGD-mediated cell death, we treated the slice cultures with MK-801 during the insult. The (+) MK-801 stereoisomer was used for all experiments as it blocks both NR2A and NR2B containing NMDARs by the same potency (similar IC_{50} values), as well as being more pH stable than the (−) MK-801 stereoisomer (Dravid et al. 2007). pH–stability is critical as the pH drops approximately one-unit to ∼6.5–6.8 during OGD by use of iCSF. The concentration of MK-801 needed to obtain good
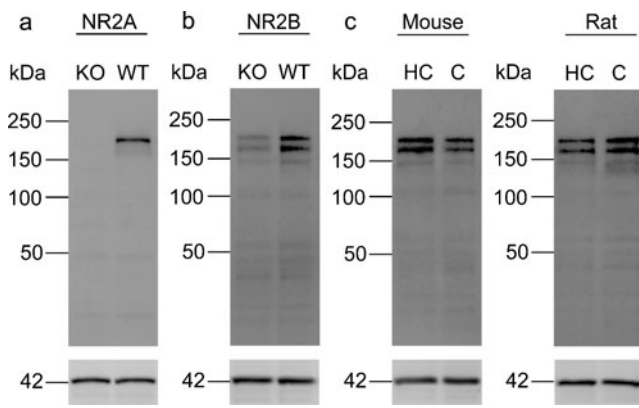
Fig. 2 Western blots confirming specificity of the *NR2A* and *NR2B* antibodies applied. **a** NR2A antibody was tested on forebrain material from adult NR2A deleted mice (*KO*) and their control littermates (*WT*). Labeling was completely abolished in the KO animal. A strong band of β-actin confirms the presence of proteins in the membrane. **b** NR2B antibodies tested on forebrain material from adult forebrain-specific conditional NR2B deleted mice (*KO*) and their control littermates (*WT*). All three bands for NR2B labeling were markedly reduced in the KO, indicating that all three bands are reflecting NR2B. See text for discussion. **c** NR2B antibody tested on hippocampal (*HC*) and cortical (*C*) material from adult wild-type mice and rats. The three bands obtained with the NR2B antibody were reproduced in extracts from hippocampus and cerebral cortex of both mice and rats, ruling out the possibility of species or regional differences

neuroprotection increased with time after the insult (Fig. 5). As much as 100 μM MK-801 was required to block cell death at 72 h after OGD (Fig. 5c). MK-801 at 10 μM failed to offer significant protection (Fig. 5).

NMDA induces excitotoxic cell death with equal potency when applied in combination with OGD as when applied alone

The relatively low cytoprotective potency of MK-801 in OGD could reflect inhibition of NMDARs due to the low pH that prevails during OGD. To explore this possibility, we exposed slice cultures to NMDA (200 μM) in iCSF in the anaerobic chamber (OGD). We found that cell death developed rapidly to reach a maximum about 24 h after the insult, comparable to our results obtained with exposure to NMDA alone (Figs. 3 and 6). Exposure to OGD induced the same extent of cell

Fig. 3 NMDA induces excitotoxic cell death in organotypical slice ▶ cultures that can be fully counteracted by MK-801. **a** Cell death was measured by analysis of propidium iodide (PI) fluorescence intensity. Massive cell death was apparent from 24 h after exposure to 150 μM NMDA, especially in the selective vulnerable CA1 region and sustained at 48 h (**b**) and 72 h (**c**) after treatment. Cell death could be counteracted completely by MK-801 (10–100 μM), even at the lowest concentration (*p*≤0.05). Data are presented as mean ± standard error of mean (SEM). *n*=6 in control (No NMDA) and 10 μM MK-801 group, *n*=4 in the 50 μM MK-801 group and *n*=5 in 100 μM MK-801 group

death as NMDA. However, the development of cell death was delayed and reached a maximum about 72 h after the insult (Fig. 6). Our data indicate that the low efficacy of MK-801 during OGD cannot be attributed to proton block of the NMDARs.
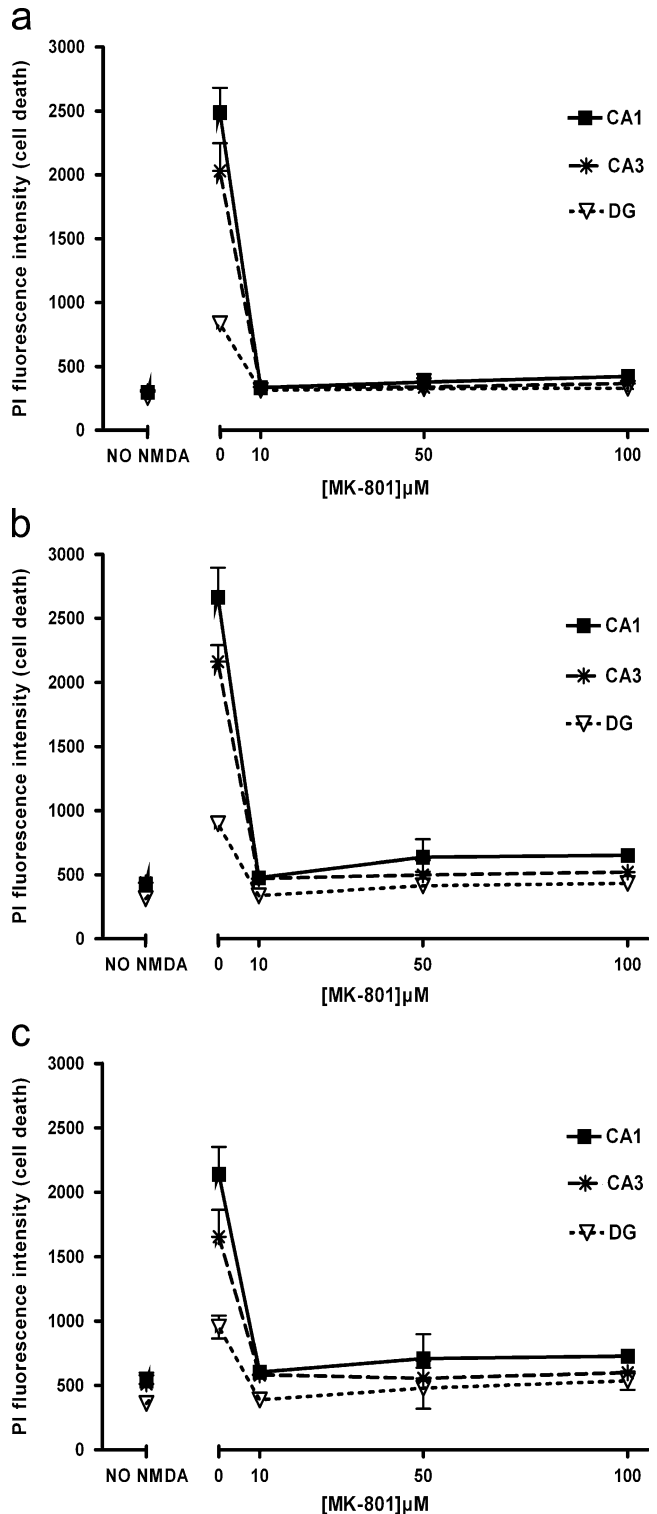
Fig. 4 Oxygen- and glucose deprivation (*OGD*) induces delayed and selective cell death in the vulnerable CA1 pyramidal cells in organotypical hippocampal slice cultures. Ischemia was induced to the slice cultures by incubation in glucose deprivated ischemic cerebral spinal fluid (iCSF) in an anaerobic chamber. Cell death was measured by propidium iodide (PI) fluorescence intensity in the different hippocampal subregions [*CA1*, *CA3* and dentate gyrus (*DG*)], with selective labeling in the CA region (**a**). Cell death appeared around 24 h after OGD and increased towards 72 h, before a flattening of the curve towards 144 h (**b**). The drop in the curve between 96 and 144 h is probably due to fluorescence bleaching. Cell death was delayed and most pronounced in the selective vulnerable CA1 region. Data are presented as mean ± SEM., *n*=10 slices from 4 animals per group. *Scale bar* 0.5 mm
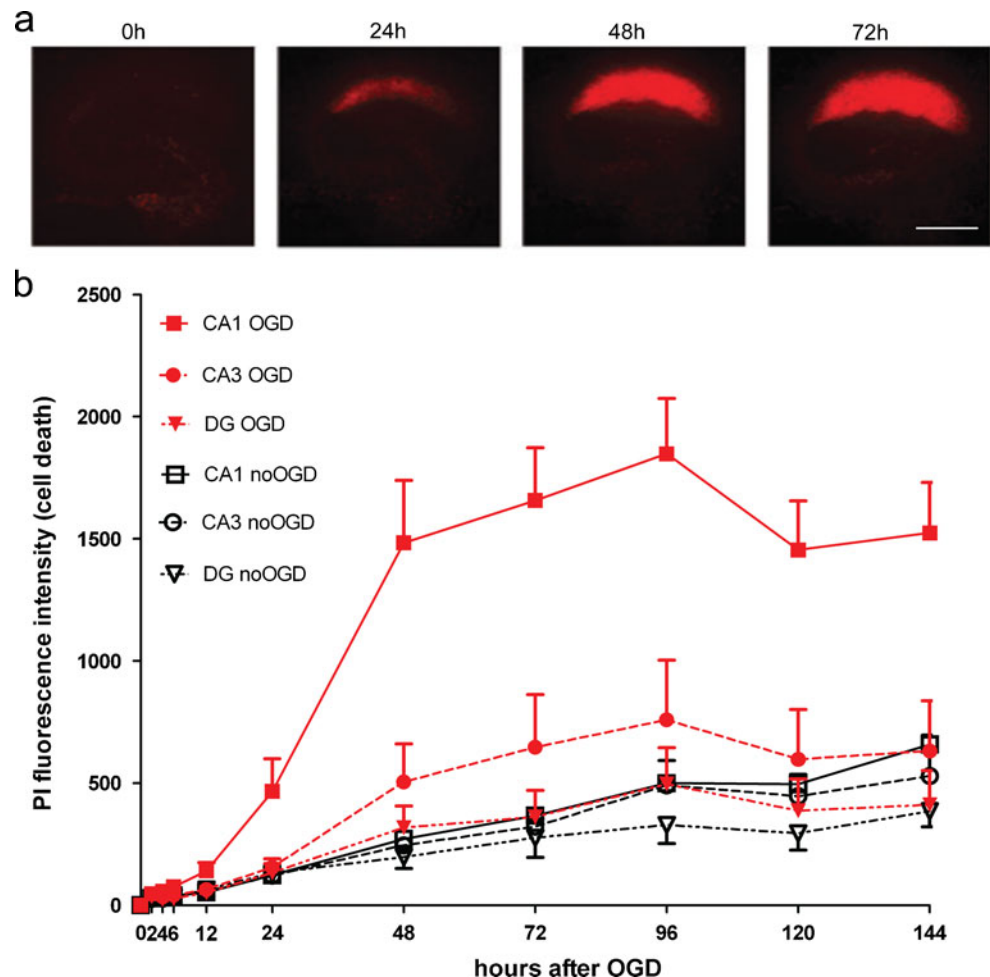
No significant changes in mRNA levels of NR1, NR2A or NR2B after OGD

Next, we wanted to resolve if the low potency of MK-801 in counteracting OGD-induced cell death could be due to an early down-regulation of the NMDARs after OGD, implying increased contribution of alternative excitotoxic signaling pathways. We investigated mRNA levels of the NMDAR subunits NR1, NR2A and NR2B at different time points (1, 3, 4 and 24 h) after the ischemic insult with corresponding control groups (Fig. 7a–c). Thus analysis was performed prior to development of significant cell death. None of the NMDAR subunits displayed statistically significant changes in mRNA level after OGD (Fig. 7a–c). The values were standardized to GAPDH and normalized to the control group for each time point.

Discussion

Our study is the first comparative evaluation of NMDARs as mediators of NMDA- and OGD-induced cell death in organotypical hippocampal slice cultures. Our data show that the key subunits NR1, NR2A and NRB are expressed in cultured slices but that they are down-regulated in the first time period after slice preparation (Fig. 1a–c). This is probably an effect of the slice preparation per se and justifies the common practice of allowing slice cultures to mature for ~14 days before experimental manipulations. Thus, slice cultures represent an advantage over acute slices, as the slice cultures will have recovered from the stress and damage introduced by slice preparation at the time they are used in experimental settings. Our data are in line with results from a study on organotypical hippocampal slices cultivated on membranes (Stoppini et al.1991), demonstrating a postnatal age-related change in NR2A and NR2B subunits composition that parallels what is seen in vivo in rodents (Wise-Faberowski et al., 2009). In our study, we additionally investigated the total level of NMDAR indicated by NR1 expression. Wise-Faberowski et al. also found that NMDAR subunit composition was dependent upon duration of OGD in their model.

Our study shows that the NMDARs are functional in the sense that NMDA application rapidly induces cell damage that can be effectively blocked by 10 μM MK-801

a

b

c
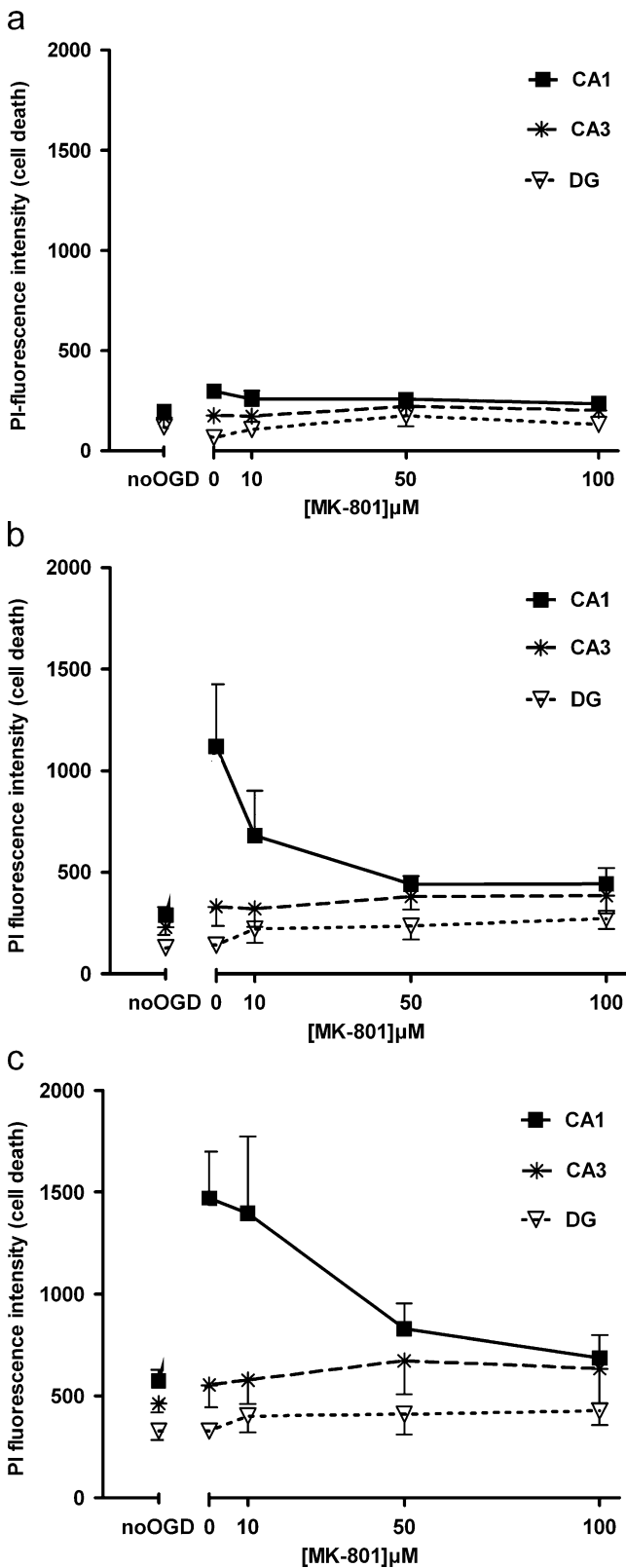
(Fig. 3a–c). This finding provides a baseline for assessing the extent to which NMDARs contribute to OGD-induced cell death. MK-801 at 10 μM was not sufficient to offer

◀ **Fig. 5** Oxygen and glucose deprivation (OGD) induce cell death that can only be partially counteracted by 10 μM MK-801. OGD induced delayed and CA1-selective cell death that appear at 24 h (**a**) and aggravates towards 48 h (**b**) and 72 h (**c**) after the insult; 10 μM MK-801 only partially counteracted OGD-induced cell death (**a–c**). At 48 h (**b**) and 72 h (**c**), very high concentrations of MK-801 (50–100 μM) were needed to obtain almost full neuroprotection ($p<0.05$). MK-801 showed a lack in potency with time after OGD. Data are presented as mean ± SEM, $n=5$ slices in each group, except the 100 μM MK-801 group were $n=6$

cytoprotection after OGD and as much as 100 μM was required to obtain full protection at 72 h (Fig. 5c). The relatively low efficacy of MK-801 post-OGD is not due to the reduced transcription of NMDAR genes, as judged by RT-PCR analyses (Fig. 7b). The low efficacy could be due to inhibition of NMDAR responses caused by low pH of the incubation medium (Tang et al. 1990), as pH in the medium was kept low to mimic the conditions in brain ischemia in vivo. However, we found that NMDA induced excitotoxic cell death in the slice cultures with the same potency during ischemic conditions and lowered pH as during physiological pH (Figs. 3 and 6). It has been shown in recombinant NMDARs that by lowering the pH from 7.6 to 6.9, NR2A (but not NR2B) is inhibited, displaying reduced opening probability and opening time of the channel. A concomitant increased association rate and strong increase in potency was demonstrated for (−)MK-801 but not for (+)MK-801. However, for (+)MK-801 there
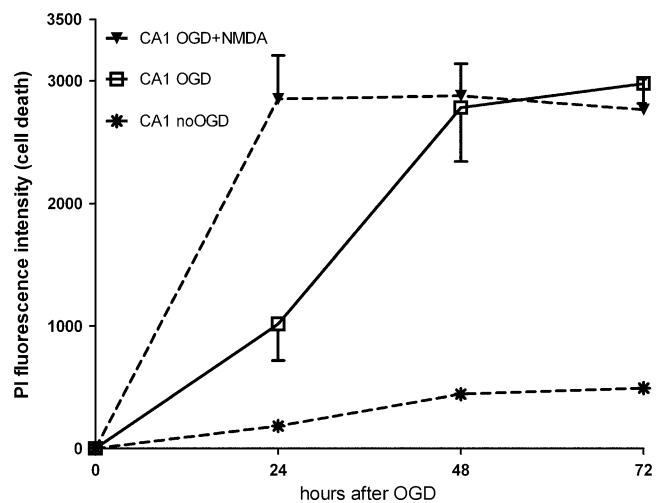

Fig. 6 NMDA receptors can be activated by NMDA to the same extent at ischemic low pH as at physiological pH. Oxygen and glucose deprivation (OGD) was performed in an anaerobic incubator and the slices were incubated in ischemic cerebral spinal fluid (iCSF). Cell death was measured by propidium iodide (PI) fluorescence intensity. Exposure to NMDA (200 μM) during OGD rapidly induced cell death in the CA1 region, with maximum cell death already at 24 h after OGD. OGD induced more delayed cell death but reached with time the same level as with NMDA. Data are presented as mean ± SEM., $n=4$ slices in the noOGD (control) group and in the OGD + NMDA group, $n=5$ slices in the OGD group. The slices were prepared from 4 animals
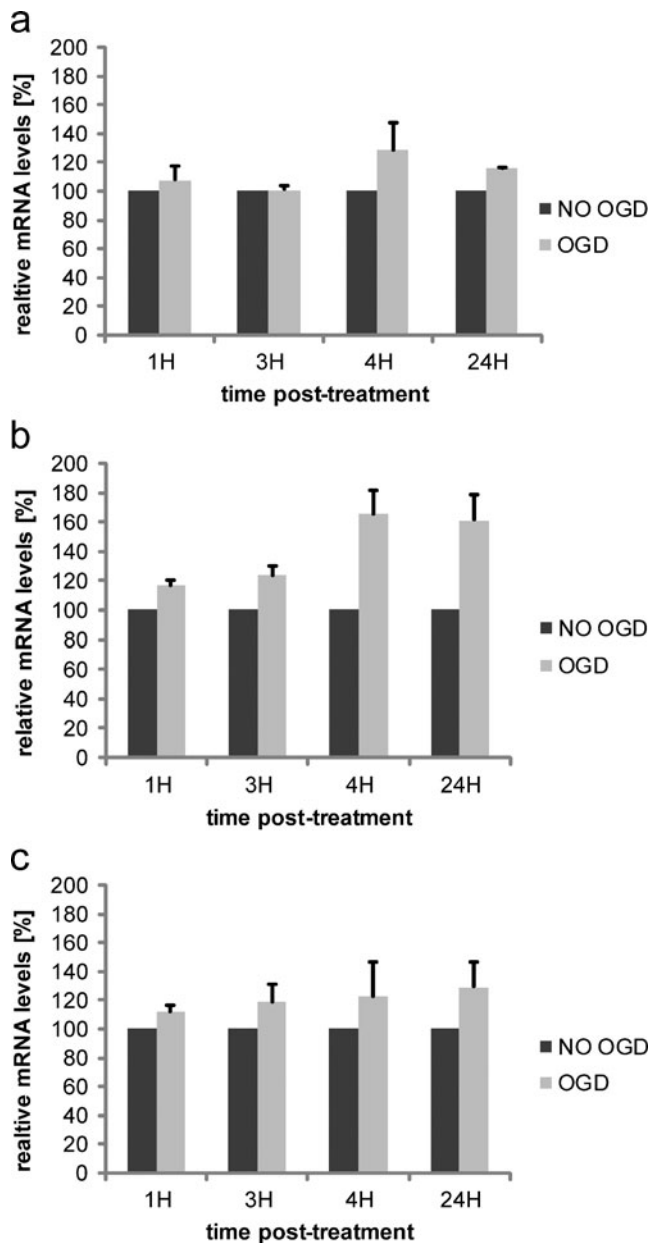
Fig. 7 mRNA levels for NR1, NR2A and NR2B are not changed after oxygen and glucose deprivation (OGD). mRNA isolated from organotypical slice cultures subjected to OGD or only to aCSF (noOGD) analyzed with real-time PCR TaqMan. The graphs represent results from one experiment in three individual runs. NMDA receptor Ct-values are standardized to GAPDH control assay. The OGD groups are standardized to the NO OGD control at respective time-points. **a** Relative mRNA levels of NR1 after 1, 3, 4 and 24 h after OGD (time post-treatment). **b** As in (**a**) but relative mRNA levels of the NR2A subunit. **c** as in (**a**) but relative mRNA levels of the NR2B subunit. For each data point, $n=4–5$ animals (4–5 slices pooled together per group). Data are presented as mean and standard error of mean (±SEM)

was no change in neuroprotective potency with decrease in pH, in contrast to (−)MK-801. The change in pH did not alter conductance of the receptor but induced a lack of

voltage-dependence for MK-801, probably due to structural change by protonization of the receptor and ease of binding of the antagonist in the pore (Dravid et al. 2007). Thus, the discrepancy in neuroprotection of (+)MK-801 induced by NMDA or OGD could not be explained by protonic inhibition of NMDARs, as NMDA was equally potent in inducing excitotoxic cell death under ischemic acidic conditions as at physiological pH. Nor could this discrepancy be explained by downregulation of genes encoding NMDAR subunit proteins.

When taken together, our data indicate that while NMDARs certainly contribute to post-OGD damage, there must be co-activation of other cell death pathways whose relative significance might increase as a consequence of the lowered pH. Many receptors and channels are activated by changes in pH, including transient receptor potential (TRP) channels and acid sensing ion channels (ASICs). These and other receptors and channels may couple to important signaling pathways in OGD and operate in parallel with classic excitotoxic signaling (Szydlowska and Tymianski 2010). Involvement of multiple pathways may be part of the explanation why NMDAR antagonists have failed in clinical trials. A combination therapy using blockers of several routes of Ca^{2+}-influx might be necessary to obtain neuroprotection in stroke (Szydlowska and Tymianski 2010; Cook and Tymianski 2011). Organotypical hippocampal slice cultures represent a good model for studying mechanisms underlying cell death signaling in brain ischemia. The model is independent of systemic parameters and allows control of the microenvironment and experimental manipulations.

In previous studies of organotypical cultures, 10 or 30 μM MK-801 was reported to offer protection (Bonde et al. 2005; Newell et al. 1995). However, in these studies, the pH of the medium was not adjusted to that typical of ischemic tissue. In earlier studies, Wieloch´s group used 20 μM MK-801 to obtain significant cytoprotection after OGD in the same model but presented data only up to 24 h after OGD (Rytter et al. 2003). In our study 50 μM MK-801 gave significant cytoprotection also at 48 h after OGD. None of the previous studies included post-OGD observation periods as long as 72 h and therefore one can only speculate if the concentration of MK-801 required for protection would have increased as a function of time as seen in the present study.

A previous analysis in organotypical hippocampal slice cultures reported an immediate down-regulation of mRNA levels of all NMDAR subunits after OGD, with partial recovery after 3 h. This contrasts with the present results. It is important to take into consideration that Dos-Anjos et al. (2009) prolonged the OGD to 30 min in order to obtain an immediate and non-CA1 specific cell death, whereas we limited OGD to ~15 min to ensure a delayed and CA1-specific cell death. Hence, the two studies are not directly comparable.

In conclusion, while NMDARs contribute to OGD-induced cell death in organotypical slice cultures, additional mechanisms are also at play. We believe that the significance of these additional mechanisms increases at long observation times and that this must be compensated for by a more complete blockade of NMDA receptors. Reflecting on the multiplicity of mechanisms involved, the immediate cell death response seen after NMDA application differs from the delayed response seen after OGD. L-type voltage gated Ca^{2+} channels (L-VGCCs) may contribute to delayed damage (Brewer et al. 2007). Furthermore, TRPM7–a member of the transient receptor potential family–is involved in anoxic cell death (Aarts et al. 2003) and in delayed ischemic cell death (Sun et al. 2009). Also acid sensing calcium channels (ASCC1) that are activated via NMDARs (Gao et al. 2005) and purinergic receptors (P2X) (Runden-Pran et al. 2005) are candidates worth considering. Both are activated by parameters, respectively pH and ATP production, which are affected during stimulated ischemia in vivo (Nedergaard et al. 1991; Silver and Erecinska 1992). Common to activation of all these receptors and channels, as well as NMDARs, is contribution to an increased intracellular level of Ca^{2+}, which can trigger a range of downstream neurotoxic cascades, including mitochondrial uncoupling and activation of calpains, proteases, protein kinases and endonucleases (Szydlowska and Tymianski 2010). Besides the intracellular level of Ca^{2+}, the route of Ca^{2+} entry (from extra- or intracellular stores) determines the subsequent toxicity (Sattler et al. 2000; Szydlowska and Tymianski 2010). Some routes, as NMDARs, are clearly associated with Ca^{2+}-dependent cell death signaling, while other routes of entry do not elicit cell death. Mitochondrial dysfunction due to Ca^{2+}-influx via overstimulated glutamate receptors and Ca^{2+} overload is an early event in excitotoxic cell death and can be coupled to ROS formation and release of apoptotic factors (Szydlowska and Tymianski 2010). Oxidative stress and ROS can induce damage to DNA and other macromolecules. We have shown previously in this model that there is a reduced capacity for base excision repair of oxidative DNA damage in the vulnerable CA1 (Rolseth et al. 2008).

Our results validate the use of organotypical hippocampal slice cultures as an ex vivo model to investigate brain ischemia based on expression, functionality and stability of the NMDAR subunits.

References

Aamodt SM, Constantine-Paton M (1999) The role of neural activity in synaptic development and its implications for adult brain function. Adv Neurol 79:133–144

Aarts M, Iihara K, Wei WL, Xiong ZG, Arundine M, Cerwinski W, MacDonald JF, Tymianski M (2003) A key role for TRPM7 channels in anoxic neuronal death. Cell 115:863–877

Arundine M, Tymianski M (2003) Molecular mechanisms of calcium-dependent neurodegeneration in excitotoxicity. Cell Calcium 34:325–337

Benveniste H, Drejer J, Schousboe A, Diemer NH (1984) Elevation of the extracellular concentrations of glutamate and aspartate in rat hippocampus during transient cerebral ischemia monitored by intracerebral microdialysis. J Neurochem 43:1369–1374

Bliss TV, Collingridge GL (1993) A synaptic model of memory: long-term potentiation in the hippocampus. Nature 361:31–39

Bonde C, Noraberg J, Noer H, Zimmer J (2005) Ionotropic glutamate receptors and glutamate transporters are involved in necrotic neuronal cell death induced by oxygen-glucose deprivation of hippocampal slice cultures. Neuroscience 136:779–794

Brewer LD, Thibault O, Staton J, Thibault V, Rogers JT, Garcia-Ramos G, Kraner S, Landfield PW, Porter NM (2007) Increased vulnerability of hippocampal neurons with age in culture: temporal association with increases in NMDA receptor current, NR2A subunit expression and recruitment of L-type calcium channels. Brain Res 1151:20–31

Camacho A, Massieu L (2006) Role of glutamate transporters in the clearance and release of glutamate during ischemia and its relation to neuronal death. Arch Med Res 37:11–18

Choi DW (1992) Excitotoxic cell death. J Neurobiol 23:1261–1276

Clark AJ, Bissinger P, Bullock DW, Damak S, Wallace R, Whitelaw CB, Yull F (1994) Chromosomal position effects and the modulation of transgene expression. Reprod Fertil Dev 6:589–598

Cook DJ, Tymianski M (2011) Translating promising preclinical neuroprotective therapies to human stroke trials. Expert Rev Cardiovasc Ther 9:433–449

Dos-Anjos S, Martinez-Villayandre B, Montori S, Perez-Garcia CC, Fernandez-Lopez A (2009) Early modifications in N-methyl-D-aspartate receptor subunit mRNA levels in an oxygen and glucose deprivation model using rat hippocampal brain slices. Neuroscience 164:1119–1126

Dravid SM, Erreger K, Yuan H, Nicholson K, Le P, Lyuboslavsky P, Almonte A, Murray E, Mosely C, Barber J, et al. (2007) Subunit-specific mechanisms and proton sensitivity of NMDA receptor channel block. J Physiol 581:107–128

Gähwiler BH, Capogna M, Debanne D, McKinney RA, Thompson SM (1997) Organotypic slice cultures: a technique has come of age. Trends Neurosci 20:471–477

Gambrill AC, Barria A (2011) NMDA receptor subunit composition controls synaptogenesis and synapse stabilization. Proc Natl Acad Sci USA 108:5855–5860

Gao J, Duan B, Wang DG, Deng XH, Zhang GY, Xu L, Xu TL (2005) Coupling between NMDA receptor and acid-sensing ion channel contributes to ischemic neuronal death. Neuron 48:635–646

Hardingham GE, Fukunaga Y, Bading H (2002) Extrasynaptic NMDARs oppose synaptic NMDARs by triggering CREB shut-off and cell death pathways. Nat Neurosci 5:405–414

Hardingham GE, Bading H (2010) Synaptic versus extrasynaptic NMDA receptor signalling: implications for neurodegenerative disorders. Nat Rev Neurosci 11:682–696

Kohr G (2006) NMDA receptor function: subunit composition versus spatial distribution. Cell Tissue Res 326:439–446

Kristensen BW, Noraberg J, Zimmer J (2001) Comparison of excitotoxic profiles of ATPA, AMPA, KA and NMDA in organotypic hippocampal slice cultures. Brain Res 917:21–44

Laake JH, Haug FM, Wieloch T, Ottersen OP (1999) A simple in vitro model of ischemia based on hippocampal slice cultures and propidium iodide fluorescence. Brain Res Brain Res Protoc 4:173–184

Lipton SA, Rosenberg PA (1994) Excitatory amino acids as a final common pathway for neurologic disorders. N Engl J Med 330:613–622

Liu Y, Wong TP, Aarts M, Rooyakkers A, Liu L, Lai TW, Wu DC, Lu J, Tymianski M, Craig AM, et al. (2007) NMDA receptor subunits have differential roles in mediating excitotoxic neuronal death both in vitro and in vivo. J Neurosci 27:2846–2857

Malenka RC, Nicoll RA (1999) Long-term potentiation–a decade of progress? Science 285:1870–1874

Martel MA, Wyllie DJ, Hardingham GE (2009) In developing hippocampal neurons, NR2B-containing N-methyl-D-aspartate receptors (NMDARs) can mediate signaling to neuronal survival and synaptic potentiation, as well as neuronal death. Neuroscience 158:334–343

Martinez-Sanchez M, Striggow F, Schroder UH, Kahlert S, Reymann KG, Reiser G (2004) Na(+) and Ca(2+) homeostasis pathways, cell death and protection after oxygen-glucose-deprivation in organotypic hippocampal slice cultures. Neuroscience 128:729–740

Milnerwood AJ, Gladding CM, Pouladi MA, Kaufman AM, Hines RM, Boyd JD, Ko RW, Vasuta OC, Graham RK, Hayden MR, Murphy TH, Raymond LA (2010) Early increase in extrasynaptic NMDA receptor signaling and expression contributes to phenotype onset in Huntington's disease mice. Neuron 65:178–190

Montero M, Poulsen FR, Noraberg J, Kirkeby A, van Beek J, Leist M, Zimmer J (2007) Comparison of neuroprotective effects of erythropoietin (EPO) and carbamylerythropoietin (CEPO) against ischemia-like oxygen-glucose deprivation (OGD) and NMDA excitotoxicity in mouse hippocampal slice cultures. Exp Neurol 204:106–117

Monyer H, Sprengel R, Schoepfer R, Herb A, Higuchi M, Lomeli H, Burnashev N, Sakmann B, Seeburg PH (1992) Heteromeric NMDA receptors: molecular and functional distinction of subtypes. Science 256:1217–1221

Monyer H, Burnashev N, Laurie DJ, Sakmann B, Seeburg PH (1994) Developmental and regional expression in the rat brain and functional properties of four NMDA receptors. Neuron 12:529–540

Moriyoshi K, Masu M, Ishii T, Shigemoto R, Mizuno N, Nakanishi S (1991) Molecular cloning and characterization of the rat NMDA receptor. Nature 354:31–37

Nedergaard M, Kraig RP, Tanabe J, Pulsinelli WA (1991) Dynamics of interstitial and intracellular pH in evolving brain infarct. Am J Physiol 260:R581–588

Newell DW, Barth A, Papermaster V, Malouf AT (1995) Glutamate and non-glutamate receptor mediated toxicity caused by oxygen and glucose deprivation in organotypic hippocampal cultures. J Neurosci 15:7702–7711

Noraberg J, Jensen CV, Bonde C, Montero M, Nielsen JV, Jensen NA, Zimmer J (2007) The developmental expression of fluorescent proteins in organotypic hippocampal slice cultures from transgenic mice and its use in the determination of excitotoxic neurodegeneration. Altern Lab Anim 35:61–70

Noraberg J, Kristensen BW, Zimmer J (1999) Markers for neuronal degeneration in organotypic slice cultures. Brain Res Brain Res Protoc 3:278–290

Olney JW (1969) Brain lesions, obesity, and other disturbances in mice treated with monosodium glutamate. Science 164:719–721

Ring A, Tanso R, Noraberg J (2010) The use of organotypic hippocampal slice cultures to evaluate protection by non-competitive NMDA receptor antagonists against excitotoxicity. Altern Lab Anim 38:71–82

Rolseth V, Runden-Pran E, Neurauter CG, Yndestad A, Luna L, Aukrust P, Ottersen OP, Bjoras M (2008) Base excision repair activities in organotypic hippocampal slice cultures exposed to oxygen and glucose deprivation. DNA Repair (Amst) 7:869–878

Rossi DJ, Oshima T, Attwell D (2000) Glutamate release in severe brain ischaemia is mainly by reversed uptake. Nature 403:316–321

Runden-Pran E, Haug FM, Storm JF, Ottersen OP (2002) BK channel activity determines the extent of cell degeneration after oxygen and glucose deprivation: a study in organotypical hippocampal slice cultures. Neuroscience 112:277–288

Runden-Pran E, Tanso R, Haug FM, Ottersen OP, Ring A (2005) Neuroprotective effects of inhibiting N-methyl-D-aspartate receptors, P2X receptors and the mitogen-activated protein kinase cascade: a quantitative analysis in organotypical hippocampal slice cultures subjected to oxygen and glucose deprivation. Neuroscience 136:795–810

Runden E, Seglen PO, Haug FM, Ottersen OP, Wieloch T, Shamloo M, Laake JH (1998) Regional selective neuronal degeneration after protein phosphatase inhibition in hippocampal slice cultures: evidence for a MAP kinase-dependent mechanism. J Neurosci 18:7296–7305

Rytter A, Cronberg T, Asztely F, Nemali S, Wieloch T (2003) Mouse hippocampal organotypic tissue cultures exposed to in vitro "ischemia" show selective and delayed CA1 damage that is aggravated by glucose. J Cereb Blood Flow Metab 23:23–33

Sakimura K, Kutsuwada T, Ito I, Manabe T, Takayama C, Kushiya E, Yagi T, Aizawa S, Inoue Y, Sugiyama H (1995) Reduced hippocampal LTP and spatial learning in mice lacking NMDA receptor epsilon 1 subunit. Nature 373:151–155

Sattler R, Xiong Z, Lu WY, MacDonald JF, Tymianski M (2000) Distinct roles of synaptic and extrasynaptic NMDA receptors in excitotoxicity. J Neurosci 20:22–33

Sheng M, Cummings J, Roldan LA, Jan YN, Jan LY (1994) Changing subunit composition of heteromeric NMDA receptors during development of rat cortex. Nature 368:144–147

Silver IA, Erecinska M (1992) Ion homeostasis in rat brain in vivo: intra- and extracellular $[Ca^{2+}]$ and $[H^+]$ in the hippocampus during recovery from short-term, transient ischemia. J Cereb Blood Flow Metab 12:759–772

Stanika RI, Pivovarova NB, Brantner CA, Watts CA, Winters CA, Andrews SB (2009) Coupling diverse routes of calcium entry to mitochondrial dysfunction and glutamate excitotoxicity. Proc Natl Acad Sci U S A 106:9854–9859

Stoppini L, Buchs PA, Muller D (1991) A simple method for organotypic cultures of nervous tissue. J Neurosci Methods 37:173–182

Sun HS, Jackson MF, Martin LJ, Jansen K, Teves L, Cui H, Kiyonaka S, Mori Y, Jones M, Forder JP, et al. (2009) Suppression of hippocampal TRPM7 protein prevents delayed neuronal death in brain ischemia. Nat Neurosci 12:1300–1307

Szydlowska K, Tymianski M (2010) Calcium, ischemia and excitotoxicity. Cell Calcium 47:122–129

Tang CM, Dichter M, Morad M (1990) Modulation of the N-methyl-D-aspartate channel by extracellular H+. Proc Natl Acad Sci U S A 87:6445–6449

von Engelhardt J, Doganci B, Jensen V, Hvalby O, Gongrich C, Taylor A, Barkus C, Sanderson DJ, Rawlins JN, Seeburg PH, Bannerman DM, Monyer H (2008) Contribution of hippocampal and extra-hippocampal NR2B-containing NMDA receptors to performance on spatial learning tasks. Neuron 60:846–860

Wise-Faberowski L, Robinson PN, Rich S, Warner DS (2009) Oxygen and glucose deprivation in an organotypic hippocampal slice model of the developing rat brain: the effect on *N*-methyl-*D*-aspartate subunit composition. Anesth Analg 109:205–210

Zhang SJ, Steijaert MN, Lau D, Schutz G, Delucinge-Vivier C, Descombes P, Bading H (2007) Decoding NMDA receptor signaling: identification of genomic programs specifying neuronal survival and death. Neuron 53:549–562

Zhang SJ, Buchthal B, Lau D, Hayer S, Dick O, Schwaninger M, Veltkamp R, Zou M, Weiss U, Bading H (2011) A signaling cascade of nuclear calcium-CREB-ATF3 activated by synaptic NMDA receptors defines a gene repression module that protects against extrasynaptic NMDA receptor-induced neuronal cell death and ischemic brain damage. J Neurosci 31:4978–4990

Zhang SJ, Steijaert MN, Lau D, Schutz G, Delucinge-Vivier C, Descombes P, Bading H (2007) Decoding NMDA receptor signaling: identification of genomic programs specifying neuronal survival and death. Neuron 53:549–562

Zhou M, Baudry M (2006) Developmental changes in NMDA neurotoxicity reflect developmental changes in subunit composition of NMDA receptors. J Neurosci 26:2956–2963